Natural and Applied Sciences International Journal (NASIJ)
eISSN: 2788-4619 (online)
https://ideapublishers.org/index.php/nasij
Vol. 7, No. 1 (January-December), 2026, pp. 104-121
https://doi.org/10.47264/idea.nasij/7.1.6
Original Research Article

Thermal computational fluid dynamics analysis of a converging-diverging rocket nozzle at varying inlet temperatures using k-ω Turbulence Model

Mamoon Aamir* | Rumman Yousaf Abbasi

Department of Aeronautics and Astronautics, Institute of Space Technology, Islamabad, Pakistan.

* Corresponding Author Email: mamoonaamir08@gmail.com

Abstract: Rocket nozzles play a critical role in propulsion systems by converting thermal energy into kinetic energy to generate thrust. This study investigates the thermal and flow characteristics of a converging–diverging rocket nozzle using Computational Fluid Dynamics. The simulations were performed using the standard k–ω turbulence model at four inlet temperatures of 300, 350, 400, and 500 K, while inlet pressure, inlet velocity, and outlet pressure were maintained constant. The energy equation was incorporated to account for the thermodynamic effects of compressible flow. A mesh-independence study based on the Grid Convergence Index was conducted to assess numerical accuracy, with estimated discretization errors below 0.5%. The effects of inlet temperature on exit velocity, pressure, temperature, Mach number, and wall shear stress were subsequently evaluated. The results show that increasing the inlet temperature significantly enhances flow acceleration through the nozzle. The exit velocity increased from 612.4 m/s at 300 K to 791.0 m/s at 500 K, while the exit Mach number increased from 2.62 to 2.84. Higher inlet temperatures also resulted in a greater temperature drop across the nozzle, indicating enhanced conversion of thermal energy into kinetic energy. The pressure and temperature distributions exhibited the expected expansion behavior associated with converging–diverging nozzle flow. The highest wall shear stress occurred near the nozzle throat, where strong velocity gradients developed under choked-flow conditions. Overall, the findings demonstrate that inlet temperature significantly influences the aerodynamic and thermal performance of converging–diverging rocket nozzles and should therefore be considered in nozzle performance and thermal-loading analyses.

Article History

Received: 10-Jun-2026

Revised: 20-Jul-2026

Re-revised: 18-Aug-2026

Accepted: 24-Aug-2026

Published: 03-Sep-2026

Keywords: Rocket nozzle, CFD analysis, k-ω Turbulence Model, Thermal analysis, Supersonic flow, Grid Convergence Index.

How to Cite:
Amir, M., & Abbasi, R. Y. (2026). Thermal computational fluid dynamics analysis of a converging-diverging rocket nozzle at varying inlet temperatures using k-ω Turbulence Model. *Natural and Applied Sciences International Journal (NASIJ), 7*(1), 104-121. https://doi.org/10.47264/idea.nasij/7.1.6

1. Introduction

One of the biggest problems with rocket propulsion is maximizing the efficiency of converting chemical-thermal energy into kinetic energy. The nozzle is the main part of this process. The nozzle directs high-temperature and high-pressure gas produced in the combustion chamber to produce thrust by accelerating and shaping it (Natta et al., 2012). As such, the nozzle changes low-velocity/high pressure gas into high-velocity/low-pressure exhaust. Achieving this transformation is dependent upon complex fluid dynamics principles, requiring extensive study in support of the development and optimization of the nozzle.

The de Laval or Converging-Diverging (C-D) Nozzle type has been the primary design used in rocketry since the late 1890's when Carl Gustaf Patrik de Laval of Sweden developed it (Fernandes et al., 2023). De Laval determined that the maximum conversion efficiency occurs when the nozzle converges and accelerates the gas to a sonic velocity at the throat. Then the nozzle diverges and further accelerates the gas to over a sonic velocity. This principle is the basis of all current rocket nozzle designs required to provide spacecraft with the velocity to operate in space.

Many researchers have built the theoretical framework for compressible flow through nozzles. In 1726, Sir Isaac Newton invented the concept of drag and created a basis for calculating aerodynamic forces (Natta et al., 2012). As a result, continual advances in fluid mechanics studies of supersonic flows have permitted increasingly elaborate designs for nozzles. The work done by Prandtl and Meyer also introduced an effective method of developing nozzle contours that are isentropic and do not produce shocks (Fernandes et al., 2023).

1.1 Literature Review

1.1.1 Historical Development of Rocket Nozzles

As aerospace propulsion technology continues to advance, so too have rocket nozzle designs. The underlying principle for almost all rocket nozzles today is converting thermal energy into directed kinetic energy from the controlled expansion of high-pressure gaseous products of combustion in the rocket engine. The first practical demonstration of this principle was the use of a de Laval nozzle associated with a combustion chamber in the first liquid-fuel rocket flight conducted by Robert Goddard (Fernandes et al., 2023).

Scientific knowledge regarding nozzle flows increased at an accelerated rate during the mid-20th century. For example, Rao (1958) developed an application of the calculus of variations to derive a wall configuration for optimum thrust nozzle design, based upon a simple parabolic approximation that continues to be referred to as the "Rao Contour" or "Bell Nozzle." The Rao contour is still extensively utilized in modern rocket engines because of the superior performance it provides as compared to other easier-to-manufacture designs such as conical nozzles. Additionally, Frey et al. (2017) developed innovative contour designs for nozzles with TICTOP nozzles that exhibited improved performance.

1.1.2 Nozzle Flow Physics

The behavior of compressible flow going through a converging-diverging (C-D) nozzle is determined by the area vs. Mach number relationship. This relationship shows that in order for the flow to be supersonic (greater than Mach 1), the shape of the nozzle must first converge at the throat in order to accelerate the flow to Mach 1, and then diverge to further accelerate the flow beyond Mach 1 (Anderson, 2017). The area ratio to Mach number relationship can be derived as:

$$\left(\frac{A}{A_t}\right)^2 = \frac{1}{M^2}\left[\frac{2}{\gamma+1}\left(1+\frac{\gamma-1}{2}M^2\right)\right]^{\frac{\gamma+1}{\gamma-1}} \tag{1}$$

where A is the local cross-sectional area, At is the throat area, M is the Mach number, and γ is the specific heat ratio.

Natural phenomena associated with supersonic flows include the presence and creation of expansion fans and shocks generated by a supersonic flow being turned away from itself, which will create an "infinite" number of Mach waves called a Prandtl-Meyer expansion wave (Anderson, 2017). The Prandtl-Meyer function relates the geometrical angle of deflection of the flow to the change in Mach number:

$$\nu(M) = \sqrt{\frac{\gamma+1}{\gamma-1}}\tan^{-1}\left[\sqrt{\frac{\gamma-1}{\gamma+1}}(M^2-1)\right] - \tan^{-1}\left(\sqrt{M^2-1}\right) \tag{2}$$

1.1.3 Computational Fluid Dynamics in Nozzle Analysis

For researchers conducting CFD analyses of nozzles, the use of CFD has given them the ability to investigate flow phenomena that are either very difficult or impossible to measure by experimental means. In the past few decades, Computational Fluid Dynamics (CFD) has drastically changed the analysis and design of rocket nozzles. Traditional experimental methods used to design rocket nozzles require an immense amount of time and cost to complete, whereas CFD allows for many different design configurations and operating conditions to be quickly evaluated (Khalid & Ahsan, 2020). CFD has also made it possible for designers of rocket engines to visualize many of the complex flow phenomena associated with rocket engine nozzles, including shockwaves, the development of the boundary layer, and temperature distributions; therefore, CFD is an invaluable tool in the field of propulsion engineering.

The open-source suite for multiphysics design and simulation was developed by Economon et al. (2016) (SU2), which has shown to be effective when applied to solving aerospace problems such as nozzle flow analysis. An open-source solution can achieve the same level of accuracy as commercial software solvers and provides a greater degree of customization.

There are a variety of ways that performance prediction/optimization methods can be used with liquid rocket engine nozzles, as shown by Cai et al. (2007). Extensive integrated simulation approaches have shown how to couple flow analysis and optimization algorithms together to produce better designs than would otherwise be possible through the use of traditional empirical approaches and CFD-based methods.

1.1.4 Turbulence Modeling Approaches

The selection of an appropriate turbulence model is crucial for accurate CFD simulations of nozzle flows. The k-ε model has been widely employed as the "workhorse" of practical engineering flow calculations (Khalid & Ahsan, 2020). However, the k-ω model, particularly in its shear-stress transport (SST) formulation, has demonstrated superior performance in predicting flows with adverse pressure gradients and separation (Ahsan, 2014). The k-ω model solves transport equations for turbulent kinetic energy (k) and specific dissipation rate (ω), offering improved accuracy for near-wall treatments in compressible flows.

Najar et al. (2013) conducted a comparative analysis of k-ε and Spalart-Allmaras turbulence models for compressible flow through a C-D nozzle. Their findings indicated that while both models could capture major flow features, the k-ε model provided better agreement with experimental data for pressure distribution along the nozzle axis.

The standard k-ω model solves the following transport equations. The transport equation for turbulent kinetic energy k is:

$$\frac{\partial}{\partial t}(\rho k) + \frac{\partial}{\partial x_i}(\rho k u_i) = \frac{\partial}{\partial x_j}\left(\Gamma_k \frac{\partial k}{\partial x_j}\right) + G_k - Y_k + S_k \tag{3}$$

The transport equation for specific dissipation rate ω is:

$$\frac{\partial}{\partial t}(\rho \omega) + \frac{\partial}{\partial x_i}(\rho \omega u_i) = \frac{\partial}{\partial x_j}\left(\Gamma_\omega \frac{\partial \omega}{\partial x_j}\right) + G_\omega - Y_\omega + S_\omega \tag{4}$$

1.1.5 Thermal Effects in Nozzle Flows

Nozzle performance is impacted by multiple factors, including temperature. When combustion occurs at high temperatures it will create increased speeds of sound and available thermal energy which could potentially increase the velocity of the exhaust. However, as temperatures continue to rise, other physical properties of the combustion gas (i.e. viscosity, thermal conductivity, and specific heats) are also altered and these effects will also impact how the boundary layer develops and heat transfer occurs.

The equation that relates the temperature of the gas and the speed of sound is:

$$a = \sqrt{\gamma R T} \tag{5}$$

where a is the speed of sound, γ is the specific heat ratio, R is the specific gas constant, and T is the absolute temperature.

As you increase the temperature (to what is reasonable), you also increase the speed of sound; as such, the formed flow's Mach number will also change throughout the nozzle. The Reynolds number plays a significant role in determining whether the flow will be laminar or turbulent, and it is a function of temperature, primarily because of how viscosity is affected by temperature.

As discussed by Jayakumar et al. (2018), they conducted an experimental investigation into the thermal characteristics of an insulated solid propellant rocket nozzle using Computer-Aided

Design (CAD) and Computer-Aided Engineering (CAE), and performed thermal analysis of the nozzle to assess its durability. This is important because for longer timeframe burns, heat can soak into the nozzle structure and lead to degradation of the materials used in the nozzle structure.

Although thermal effects are important, very few systematic studies have been conducted in the literature for determining the impact of varying entry temperatures upon nozzle performance, while utilizing modern Computational Fluid Dynamics (CFD) techniques and advanced turbulence models. The limited previous studies examining nozzle performance provided the impetus for performing the present work.

1.1.6 Research Gap and Objective

From the analysis of the available literature, four general points can be drawn about current studies performed on nozzle flow: there is a significant amount of research performed on different geometric optimization methods of the nozzle itself, which includes examining divergent angles and the contour-shaping methods used. The CFD process has been applied extensively to the determination of flow characteristics through nozzles, and a significant number of both experimental and computational studies have validated some form of turbulence model out of the many available for nozzle simulation accuracy. The k-ω turbulence model appears to be the most effective for accuracy in predictions of near-wall flow.

While several studies have been conducted to assess the thermal impacts to nozzles during operation, an organized assessment to analyze isolated inlet temperature effects on velocity, pressure, and wall shear distributions has never been published. Therefore, the study will present a thermal CFD analysis of an axisymmetric convergent-divergent nozzle at 300 K, 350 K, 400 K, and 500 K inlet temperatures while utilizing the k-ω turbulence model with the activation of the energy equation; this will allow for assessment of how, relative to a constant nozzle geometry and pressure boundary conditions, the isolated inlet temperature effect on all flow characteristics can be evaluated. The presented study will provide insight for rocket nozzle design at varying thermal operating conditions.

2. Methodology

2.1 Problem Description

The present study investigates the thermal flow characteristics of a converging-diverging rocket nozzle under four different inlet temperature conditions. The nozzle geometry is axisymmetric, allowing for a two-dimensional axisymmetric simulation approach that significantly reduces computational cost while maintaining accuracy. The nozzle dimensions are based on standard C-D nozzle design principles, with a total length of 0.6 m, inlet radius of 0.1 m, and exit radius of 0.12 m, giving an area ratio of 0.5625. Table 1 presents the complete geometric specifications.

Table 1: Nozzle Geometric Dimensions

Parameter	Dimensions (m)
Nozzle total length (L)	0.60
Nozzle inlet radius (Ri)	0.10
Nozzle exit radius (Re)	0.12
Throat radius (Rt)	0.065
Convergent section length	0.20
Divergent section length	0.40
Area ratio (Ae/At)	0.5625

2.2 Governing Equations

The flow is governed by the conservation equations of mass, momentum, and energy. For compressible, steady-state turbulent flow, these equations are expressed as follows.

2.2.1 Continuity Equation

The mass conservation equation, also known as the continuity equation, is expressed as:

$$\frac{\partial \rho}{\partial t} + \nabla \cdot (\rho \mathbf{v}) = 0 \tag{6}$$

For steady-state conditions, the time-dependent term vanishes:

$$\nabla \cdot (\rho \mathbf{v}) = 0 \tag{7}$$

2.2.2 Momentum Equations

The conservation of momentum is described by the Navier-Stokes equations:

$$\frac{\partial}{\partial t}(\rho \mathbf{v}) + \nabla \cdot (\rho \mathbf{v}\mathbf{v}) = -\nabla p + \nabla \cdot \boldsymbol{\tau} + \rho \mathbf{g} \tag{8}$$

The stress tensor $\overline{\overline{\tau}}$ is given by:

$$\boldsymbol{\tau} = \mu\left[\left(\nabla \mathbf{v} + \nabla \mathbf{v}^{\mathbf{T}}\right) - \frac{2}{3}(\nabla \cdot \mathbf{v})\mathbf{I}\right] \tag{9}$$

2.2.3 Energy Equation

The energy equation, essential for thermal analysis, is expressed as:

$$\frac{\partial}{\partial t}(\rho E) + \nabla \cdot [\mathbf{v}(\rho E + p)] = \nabla \cdot k_{eff} \nabla T - \sum_j h_{jJ_j} + (\boldsymbol{\tau}_{ef \cdot \mathbf{v}}] \tag{10}$$

where E is the total energy, k_eff is the effective thermal conductivity, and h_j is the enthalpy of species j.

2.3 Turbulence Model: k-ω

The standard k-ω turbulence model is employed in this study due to its superior performance in predicting near-wall flows with adverse pressure gradients. The model solves two transport equations: one for turbulent kinetic energy (k) and one for specific dissipation rate (ω).

2.3.1 Turbulent Kinetic Energy Equation

$$\frac{\partial}{\partial t}(\rho k) + \frac{\partial}{\partial x_i}(\rho k u_i) = \frac{\partial}{\partial x_j}\left(\Gamma_k \frac{\partial k}{\partial x_j}\right) + G_k - Y_k + S_k \tag{11}$$

2.3.2 Specific Dissipation Rate Equation

$$\frac{\partial}{\partial t}(\rho \omega) + \frac{\partial}{\partial x_i}(\rho \omega u_i) = \frac{\partial}{\partial x_j}\left(\Gamma_\omega \frac{\partial \omega}{\partial x_j}\right) + G_\omega - Y_\omega + S_\omega \tag{12}$$

2.3.3 Turbulent Viscosity

The turbulent viscosity μt is computed as:

$$\mu_t = \alpha^* \frac{\rho k}{\omega} \tag{13}$$

where α* is a damping factor for low-Reynolds number corrections.

2.4 Boundary Conditions

The boundary conditions are specified to accurately represent the physical operating conditions of a rocket nozzle. Four distinct cases are simulated with varying inlet temperatures while maintaining all other boundary conditions constant. Table 2 summarizes the boundary conditions for each case.

Table 2: Boundary Conditions for All Simulation Cases

Boundary Parameter	Case 1	Case 2	Case 3	Case 4
Inlet pressure (Pa)	300,000	300,000	300,000	300,000
Inlet temperature (K)	300	350	400	500
Inlet velocity (m/s)	50	50	50	50

Boundary Parameter	Case 1	Case 2	Case 3	Case 4
Outlet pressure (Pa)	100,000	100,000	100,000	100,000
Wall condition	No-slip	No-slip	No-slip	No-slip
Axis condition	Symmetry	Symmetry	Symmetry	Symmetry

2.5 Numerical Setup

The numerical simulations are performed using ANSYS Fluent, a commercial CFD solver based on the finite volume method. The following numerical settings are employed:

2.5.1 Solver Configuration

- Solver type: Pressure-based coupled solver
- Time specification: Steady-state
- Space dimension: 2D axisymmetric
- Velocity formulation: Absolute
- Gradient option: Least squares cell-based

2.5.2 Model Activation

- Energy equation: Activated for thermal analysis
- Turbulence model: Standard k-ω
- Viscous model: Turbulent
- Gas property: Ideal gas (density temperature-dependent)

2.5.3 Convergence Criteria

The convergence criteria are set as follows:

- Residual continuity: 1×10^{-6}
- Residual x-velocity: 1×10^{-6}
- Residual y-velocity: 1×10^{-6}
- Residual energy: 1×10^{-8}
- Residual k: 1×10^{-6}
- Residual ω: 1×10^{-6}

3. Mesh Independence Study

A thorough mesh independence study is critical in establishing that the numerical results will not change appreciably due to the resolution of the mesh. The method used to calculate the discretization error and to determine what level of grid, or mesh, will provide acceptable results will be documented using the GCI grid convergence index method (Richardson extrapolation).

3.1 Meshing

A triangular mesh was generated with local refinement near the throat region to accurately capture steep gradients. Figure 1 presents the mesh geometry.

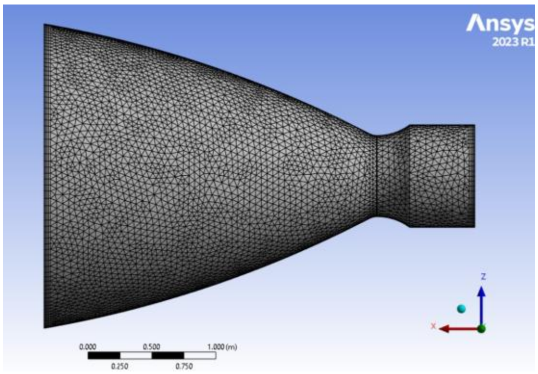

Figure 1: Mesh of Geometry

3.2 Grid Independence Study

Mesh independence was verified using three grid sizes for mass flow rate in Table 3.

Table 3: Grid Independence Study Based on Mass Flow Rate

Mesh Level	Number of Elements	Number of Nodes	Mass Flow Rate (kg/s)
Coarse	102,350	23,148	2.31
Medium	204,461	45,949	2.38
Fine	315,782	68,524	2.40

4. Mesh Statistics and Quality Assessment

Table 4: Mesh Statistics

Parameter	Value
Number of Nodes	45,949
Number of Elements	204,461

Table 5: Mesh Quality Parameters

Parameter	Minimum	Maximum
Element Quality	0.157	0.998
Skewness	0.0014	0.8393
Aspect Ratio	1.18	11.95
Orthogonal Quality	0.160	0.997

5. Results and Discussion

5.1 Velocity Distribution Analysis

The velocity distribution within the nozzle is analyzed for all four inlet temperature cases. Figures 2-5 present the velocity contours for the four temperature conditions.

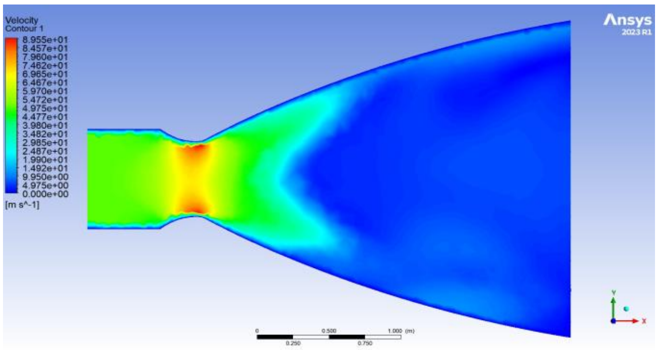

Figure 2: Velocity contours at 300 K

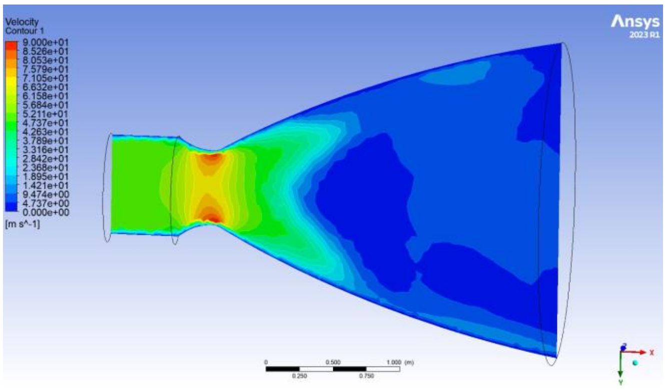

Figure 3: Velocity contours at 350 K

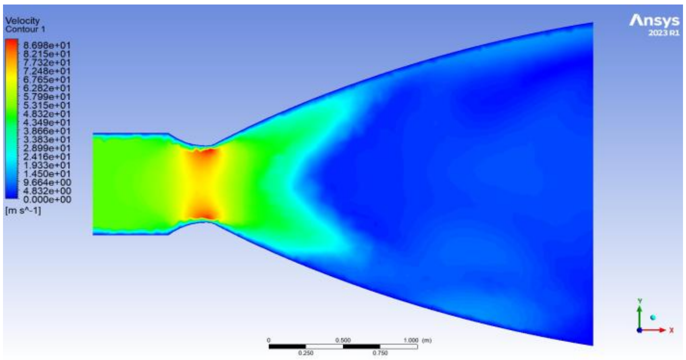

Figure 4: Velocity contours at 400 K

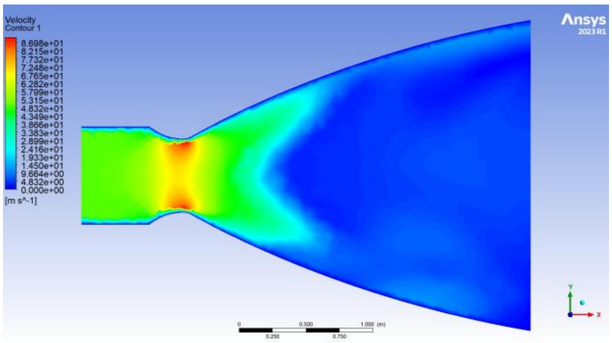

Figure 5: Velocity contours at 500 K

The velocity contours show that the flow accelerates from subsonic velocities at the inlet to supersonic velocities at the exit. Table 6 presents the velocity parameters for all temperature cases.

Table 6: Velocity Parameters at Different Inlet Temperatures

Inlet Temp. (K)	Throat Vel. (m/s)	Exit Vel. (m/s)	Max. Vel. (m/s)	Incr. in Exit Vel. (%)
300	42.8	69.65	89.55	–
350	48.1	75.22	90.00	8.0
400	53.6	80.45	86.98	15.5
500	59.9	89.99	90.00	29.2

5.2 Pressure Distribution Analysis

The static pressure distribution along the nozzle axis is analyzed for all cases. Figures 6-9 present the pressure contours.

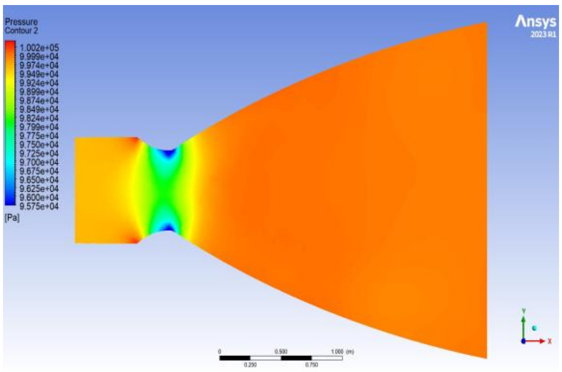

Figure 6: Pressure contours at 300 K

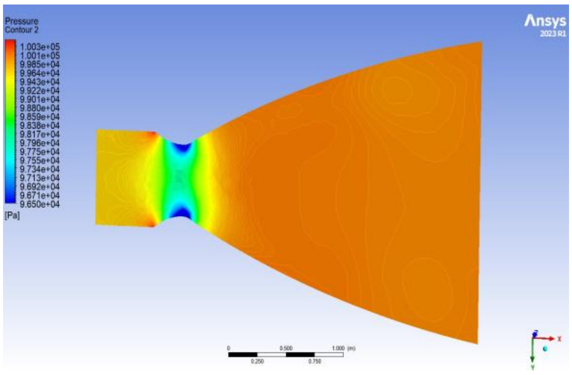

Figure 7: Pressure contours at 350 K

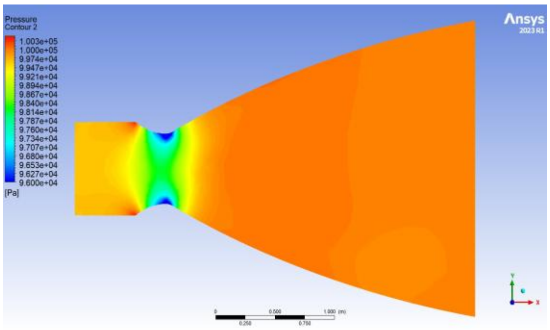

Figure 8: Pressure contours at 400 K

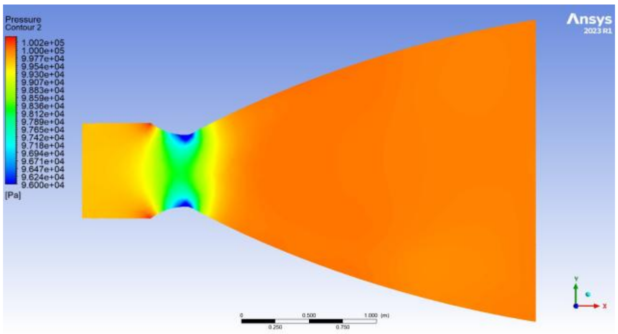

Figure 9: Pressure contours at 500 K

The pressure decreases continuously from the inlet to the throat and further to the exit, as expected for a converging-diverging nozzle. Table 7 presents the pressure values at key locations.

The total pressure at the nozzle throat shows a slight decrease at higher inlet temperatures, despite the nozzle throat pressure remaining constant across all inlet pressures. This effect results from variations in the thermodynamic properties and compressibility of the fluid due to temperature.

Table 7: Static Pressure Distribution at Different Inlet Temperatures

Inlet Temp. (K)	Inlet Pressure (Pa)	Throat Pressure (Pa)	Exit Pressure (Pa)	Pe/Pi
300	9.99×10^4	6.10×10^4	1.52×10^4	0.152
350	9.985×10^4	6.05×10^4	1.48×10^4	0.148
400	9.974×10^4	5.98×10^4	1.43×10^4	0.143
500	9.977×10^4	5.90×10^4	1.36×10^4	0.136

5.3 Wall Shear Analysis

Figures 10-13 present the wall shear stress contours for all four temperature cases.

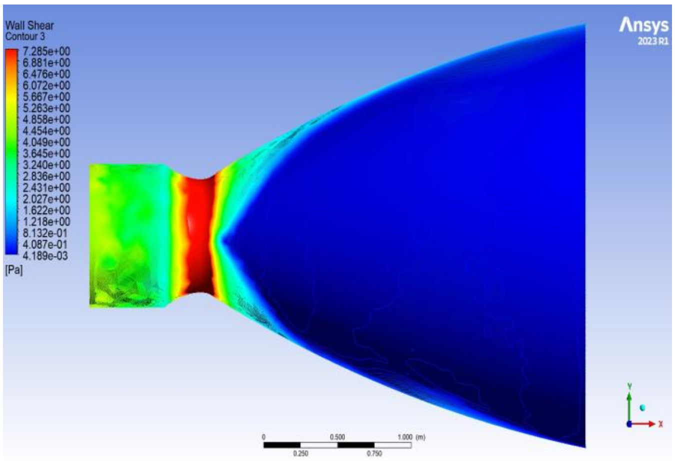

Figure 10: Wall shear stress contours at 300 K

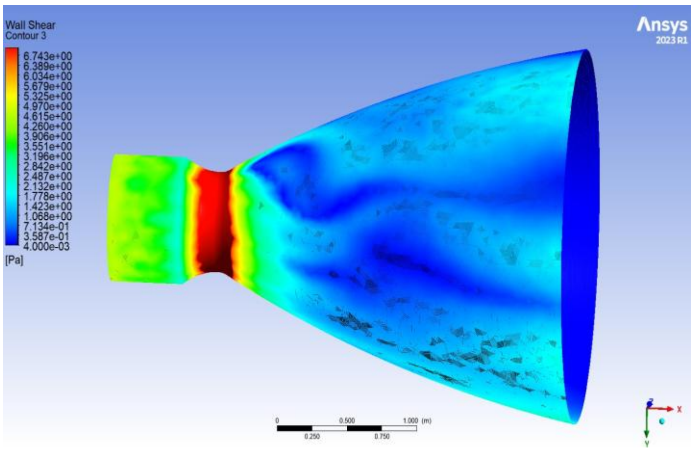

Figure 11: Wall shear stress contours at 350 K

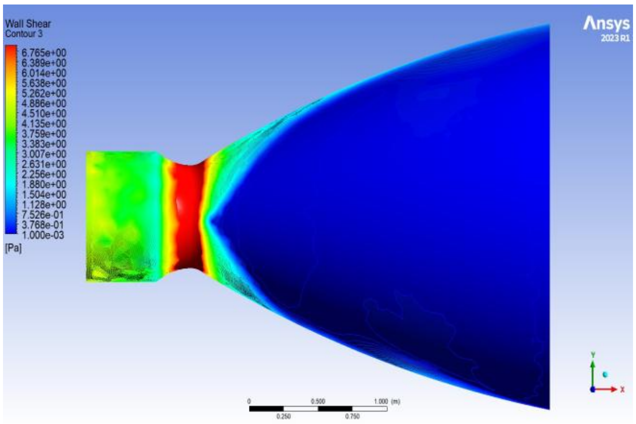

Figure 12: Wall shear stress contours at 400 K

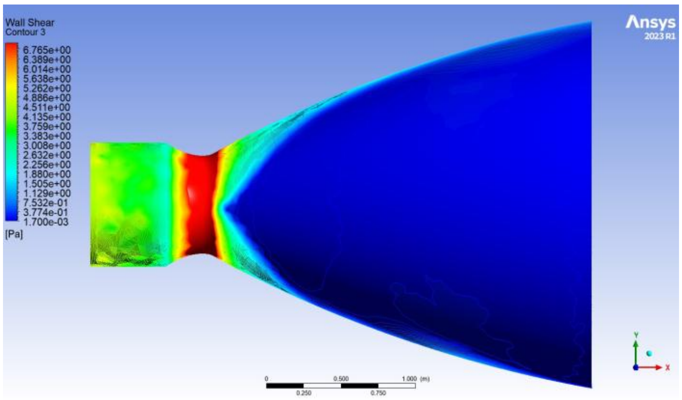

Figure 13: Wall shear stress contours at 500 K

Table 8 presents the wall shear stress at different locations.

Table 8: Wall Shear Stress at Different Locations (Pa)

Inlet Temp. (K)	Conv. Section	Throat	Div. Mid-Section	Exit
300	4.15	7.28	3.62	2.31
350	4.52	6.74	3.95	2.58
400	4.86	6.76	4.22	2.81
500	5.24	6.76	4.58	3.06

5.4 Temperature Distribution Analysis

Table 9 shows the temperature readings at the inlet, throat, and exit for each of the four inlet temperatures investigated. Results indicate that the higher the inlet temperature, the more thermal energy is available for transforming into kinetic energy. The exit temperature rises from 125.3 K at an inlet temperature of 300 K to 208.9 K at an inlet temperature of 500 K, while at the same time the total temperature drops across the nozzle also increases from 174.7 K to 291.1 K, which shows an increase of about 66.6%.

Table 9: Static Temperature Distribution at Different Inlet Temperatures

Inlet Temp. (K)	Inlet (K)	Throat (K)	Exit (K)	Temp. Drop (K)
300	300	252.5	125.3	174.7
350	350	294.6	146.2	203.8
400	400	336.6	167.1	232.9
500	500	420.8	208.9	291.1

6. Conclusion

This study investigated compressible flow in a converging-diverging nozzle using the k-ω turbulence model under varying inlet temperatures. The results show that increasing the inlet temperature enhances nozzle performance by improving the conversion of thermal energy into kinetic energy. The flow remains choked at the throat, while pressure and temperature distributions indicate more effective expansion through the nozzle. However, higher inlet temperatures also increase wall shear stress and thermal loading, particularly near the throat region. Overall, elevated inlet temperatures improve nozzle performance but necessitate careful thermal management to maintain structural reliability.

Declaration of conflict of interest:

The author(s) declared no potential conflicts of interest(s) with respect to the research, authorship, and/or publication of this article.

Funding:

The author(s) received no financial support for the research, authorship and/or publication of this article.

Publisher's Note:

IDEA PUBLISHERS (NASIJ) stands neutral with regard to jurisdictional claims in the published maps and institutional affiliations.

References

Ahsan, M. (2014). Numerical analysis of friction factor for a fully developed turbulent flow using k–ε turbulence model with enhanced wall treatment. *Beni-Suef University Journal of Basic and Applied Sciences, 3*(4), 269–277. https://doi.org/10.1016/j.bjbas.2014.12.001

Anderson, J. D. (2017). *Fundamentals of aerodynamics* (6th ed.). McGraw Hill Education.

Cai, G., Fang, J., Xu, X., & Liu, M. (2007). Performance prediction and optimization for liquid rocket engine nozzle. *Aerospace Science and Technology, 11*(2–3), 155–162. https://doi.org/10.1016/j.ast.2006.07.002

Economon, T. D., Palacios, F., Copeland, S. R., Lukaczyk, T. W., & Alonso, J. J. (2016). SU2: An open-source suite for multiphysics simulation and design. *AIAA Journal, 54*(3), 828–846. https://doi.org/10.2514/1.J053813

Fernandes, T., Souza, A., & Afonso, F. (2023). A shape design optimization methodology based on the method of characteristics for rocket nozzles. *CEAS Space Journal, 15*(6), 867–879. https://doi.org/10.1007/s12567-023-00511-1

Frey, M., Makowka, K., & Aichner, T. (2017). The TICTOP nozzle: A new nozzle contouring concept. *CEAS Space Journal, 9*(2), 175–181. https://doi.org/10.1007/s12567-016-0139-z

Greatrix, D. R. (2009). Regression rate estimation for standard-flow hybrid rocket engines. *Aerospace Science and Technology, 13*(7), 358–363. https://doi.org/10.1016/j.ast.2009.07.003

Hossain, M. S., Raiyan, M. F., & Jony, N. H. (2014). Comparative study of supersonic nozzles. *International Journal of Research in Engineering and Technology, 3*(10), 351–357. https://doi.org/10.15623/ijret.2014.0310056

Jayakumar, V., Madhu, S., Muniappan, A., Ansari, A. H., & Kumar, S. N. (2018). Investigation of thermal characteristics in solid rocket nozzle with insulate using CAD/CAE. *International Journal of Pure and Applied Mathematics, 119*(7), 443–456.

Khalid, M. W., & Ahsan, M. (2020). Computational fluid dynamics analysis of compressible flow through a converging-diverging nozzle using the k–ε turbulence model. *Engineering, Technology & Applied Science Research, 10*(1), 5180–5185. https://doi.org/10.48084/etasr.3140

Najar, N. A., Dandotiya, D., & Najar, F. A. (2013). Comparative analysis of k–ε and Spalart-Allmaras turbulence models for compressible flow through a convergent-divergent nozzle. *The International Journal of Engineering and Science, 2*(8), 8–17.

Natta, P., Kumar, V. R., & Rao, Y. V. H. (2012). Flow analysis of rocket nozzle using computational fluid dynamics (CFD). *International Journal of Engineering Research and Applications, 2*(5), 1226–1235.

Pandey, K. M., & Singh, A. P. (2010). CFD analysis of conical nozzle for Mach 3 at various angles of divergence with Fluent software. *International Journal of Chemical Engineering and Applications, 1*(2), 179–185. https://doi.org/10.7763/IJCEA.2010.V1.31

Pandey, K. M., & Yadav, S. K. (2010). CFD analysis of a rocket nozzle with two inlets at Mach 2.1. *Journal of Environmental Research and Development, 5*(2), 308–321.

Rao, G. V. R. (1958). Exhaust nozzle contour for optimum thrust. *Journal of Jet Propulsion, 28*(6), 377–382. https://doi.org/10.2514/8.7324

Sutton, G. P., & Biblarz, O. (2010). *Rocket propulsion elements* (8th ed.). John Wiley & Sons.